THE ASTROPHYSICAL JOURNAL, 265:18–25, 1983 February 1

INFRARED/OPTICAL ENERGY DISTRIBUTIONS OF HIGH-REDSHIFT QUASARS

B. T. SOIFER, G. NEUGEBAUER, J. B. OKE, K. MATTHEWS, AND J. H. LACY
Palomar Observatory, California Institute of Technology
Received 1982 April 26; accepted 1982 July 30

ABSTRACT

Measurements at 1.2, 1.6, and 2.2 μm have been combined with visual spectrophotometry of 21 quasars having redshifts $z \geq 2.66$. The primary result of this study is that the rest frame visual/ultraviolet continua of the high-redshift quasars are well described by a sum of a power-law continuum with slope ~ -0.4 and a 3000 Å bump. The rest frame visual/ultraviolet continua of these quasars are quite similar to that of 3C 273, the archetype of low-redshift quasars. There do not appear to be any significant visual/ultraviolet properties distinguishing high-redshift quasars selected via visual or radio techniques.

Subject headings: quasars — spectrophotometry

I. INTRODUCTION

Understanding of the emission mechanisms and underlying energy sources of the visual and ultraviolet continua in quasars has long been an important goal of quasar observations. The discovery of a significant number of moderately bright high-redshift quasars allows a detailed study of the rest frame ultraviolet and visual continua to be done by observing these objects at visual and near-infrared wavelengths. In this paper we report the results of such a study for 21 quasars having redshifts $z \geq 2.66$.

II. THE SAMPLE

The objects included in this study were all selected to be moderately bright ($m_v < 20$ mag) quasars with redshifts sufficiently large to bring the Lyman continuum discontinuity into the visual wavelength range. The objects are listed in Table 1. A discussion of the results of the study of the Lyman discontinuity in this sample is found in Oke and Korycansky (1982).

Fourteen objects in the present sample were discovered originally in radio surveys. The remaining seven were discovered in visual surveys; five of these were discovered in the University of Michigan objective prism survey (MacAlpine and Lewis 1978; MacAlpine, Smith, and Lewis 1977). Positions and redshifts for all the objects in this study with the exception of 1320−10 (POX 175; Kunth, Sargent, and Kowal 1981) are found in the catalog of Hewitt and Burbidge (1980). It is clear that the sample observed is not homogeneous; neither the radio nor visually selected samples obey well-defined selection criteria.

III. OBSERVATIONS

All the new observations reported here were obtained on the Hale 5.08 m telescope at Palomar Mountain. The visual observations at observed wavelengths between 3200 Å and 10,000 Å (rest wavelengths between ~800 Å and 2500 Å) were obtained with the multichannel spectrometer with bandpasses of 80 Å below 5600 Å and 160 Å above 5600 Å. These data were reported in Oke and Korycansky (1982). In the case of PKS 0528−253, multichannel observations were not available, and published observations (Smith, Jura, and Margon 1979) were used in the visual range. Because of the large air mass and small aperture (2″.8) used for the observations of PKS 0528−253, the absolute calibration has a large uncertainty, and the relative calibration may suffer from differential refraction effects (Smith, private communication). The infrared observations in the 1.25 μm, 1.65 μm, and 2.2 μm photometric bands were obtained with a solid nitrogen-cooled InSb detector. The diameter of the focal-plane aperture for all the infrared observations was 5″.

The continuum flux densities in the three infrared bands (1.25 μm, 1.65 μm, and 2.2 μm) are given in Table 1 for each quasar; at a mean redshift of 3 these correspond to rest frame wavelengths of ~0.31 μm, ~0.41 μm, and ~0.55 μm. The observations have been corrected for emission lines in the photometric bands as discussed below, and the magnitudes of these corrections are given in Table 2. The flux density at a rest wavelength of 0.174 μm obtained from the multichannel observations is also included in Table 1. In several cases infrared and visual photometry were obtained on several nights for the same object. Except as noted below, the observations agreed within their statistical uncertainties for the objects for which multiple observations were obtained, and the flux densities reported represent the average of all observations, weighted by their uncertainties.

In two cases, 0758+12, and 2351−154, the infrared photometry at one or more wavelengths suggests significant variability; in both cases there is evidence for color changes as well. The dates of observations and observed magnitudes at 1.2, 1.6, and 2.2 μm of 0758+12 and 2351−154 are given in Table 3. For 0758+12 the data at 2.2 μm indicate variability at the 99% confidence

1983ApJ...265...18S

TABLE 1

CONTINUUM FLUX DENSITIES OF HIGH-REDSHIFT QUASARS

OBJECT	OTHER NAME	z	log f_ν (mJy) λ_0 (μm) 0.174	~0.31	~0.41	~0.55	OBSERVATION DATES Visual	Infrared
0054−00	PKS	2.795	−1.10	−1.00 ± 0.04	−1.02 ± 0.06	−1.21 ± 0.12	1977 Aug	1980 Aug, 1981 Nov
0100+13	PHL 957	2.690	−0.04	+0.09 ± 0.02	+0.06 ± 0.02	−0.07 ± 0.02	1970 Oct	1976 Oct, 1979 Jul, 1979 Nov, 1981 Nov
0143−015	UM 366	3.14	−0.47	−0.35 ± 0.05	−0.31 ± 0.03	−0.35 ± 0.04	1980 Sep	1980 Oct
0143−010	UM 368	3.16	−1.17	−0.94 ± 0.12	−0.85 ± 0.05	−0.72 ± 0.06	1980 Sep, 1980 Dec	1980 Oct
0146+017	UM 141	2.91	−0.44	−0.33 ± 0.04	−0.24 ± 0.03	−0.26 ± 0.04	1980 Dec	1980 Oct
0154+045	UM 148	2.99	−0.58	−0.36 ± 0.05	−0.27 ± 0.03	−0.28 ± 0.04	1981 Jan	1980 Oct
0207+003	UM 402	2.84	−0.22	−0.04 ± 0.05	−0.05 ± 0.03	−0.08 ± 0.05	1980 Dec	1980 Oct
0528−25	PKS	2.765	−0.52	−0.43 ± 0.08	−0.28 ± 0.04	−0.36 ± 0.04	...	1980 Feb
0642+449	OH 471	3.402	−0.77	−0.53 ± 0.03	−0.51 ± 0.03	−0.50 ± 0.02	1973 Apr, 1973 Dec	1980 Feb, 1981 Nov
0758+12	MC 5	2.660	−0.94	−0.93 ± 0.03	−1.03 ± 0.03	−1.17 ± 0.04	1978 Feb	1980 Feb, 1981 Oct, 1981 Nov
0805+046	4C 05.34	2.877	−0.66	−0.50 ± 0.03	−0.43 ± 0.03	−0.55 ± 0.03	1978 Dec, 1979 Oct	1980 Feb, 1981 Nov
0830+115	MC 5	2.974	−0.77	−0.71 ± 0.04	−0.67 ± 0.03	−0.78 ± 0.04	1977 Feb	1980 Feb, 1981 Nov
0938+119	MC 5	3.190	−1.31	−1.06 ± 0.06	−1.01 ± 0.04	−1.20 ± 0.09	1977 Feb, 1977 Dec	1980 Feb, 1981 Nov
0941+261	OK 270	2.910	−0.87	−1.04 ± 0.20	−0.72 ± 0.04	−0.72 ± 0.06	1977 Feb	1980 Feb
1004+14	OL 108.1	2.707	−1.00	−0.74 ± 0.07	−0.71 ± 0.03	−0.77 ± 0.04	1977 Feb, 1977 Dec, 1978 Feb	1980 Feb
1320−10	POX 175	3.14	...	...	−0.35 ± 0.04	−0.44 ± 0.04	...	1980 Feb
1402+044	PKS	3.202	−1.22	...	−1.04 ± 0.08	−0.97 ± 0.10	1978 Jul	1980 Feb, 1980 Mar
1442+101	OQ 172	3.53	−0.49	−0.38 ± 0.07	−0.47 ± 0.04	−0.43 ± 0.05	1973 Jul	1980 Jul
2126−158	PKS	3.270	−0.11	−0.00 ± 0.02	+0.05 ± 0.02	−0.04 ± 0.02	1978 Jul	1978 Jul, 1981 Aug, 1981 Nov
2256+017	PKS	2.663	−0.97	−0.74 ± 0.03	−0.80 ± 0.02	−0.92 ± 0.04	1978 Dec	1980 Jul, 1981 Oct, 1981 Nov
2351−154	OZ 187	2.665	...	−0.30 ± 0.02	−0.27 ± 0.02	−0.30 ± 0.02	...	1980 Jul, 1981 Oct, 1981 Nov

TABLE 2

CORRECTIONS TO OBSERVED FLUX DENSITIES FOR EMISSION LINES

	CORRECTION[a]		
	WAVELENGTH (μm)		
OBJECT	1.25	1.65	2.2
0100+13	...	0.04	0.06[b]
0143−015	...	...	0.03[c]
0143−010	0.02	...	0.04[c]
0528−25	...	0.01	...
0642+449	...	...	0.07[c]
0758+12	...	0.05	0.12[b]
0938+119	0.02	...	0.05[c]
1004+14	...	0.03	0.07[b]
1320−10	...	...	0.03[c]
1402+044	...	...	0.05[c]
1442+101	...	...	0.07[c]
2126−158	...	...	0.01[c]
2256+017	...	0.06	0.12[b]
2351−154	...	0.05	0.12[b]

[a] Corrections are log (f_ν [observed]/f_ν [corrected]).
[b] Corrected for Hα in bandpass.
[c] Corrected for Hβ + [O III] $\lambda\lambda$4959, 5007 in bandpass.

level, while the data at other wavelengths do not show evidence for such variability. For 2351−154 the data at all three wavelengths show strong evidence for variability, with a total variation of 1.5 mag at 2.2 μm. Indeed it is clear that this quasar varied by $\sim$30% over the one month period of 1981 October/November. In this case there is marginal evidence for a color change with the variation, the 1.6–2.2 μm color changing by 0.4 $\pm$ 0.2 mag between 1980 July and 1981 November.

The infrared continuum observations are affected to some extent by inclusion of strong emission lines in the bandpasses of the observations. The strongest lines in the spectra of quasars that affect the continuum fluxes are Hα, Hβ, [O III] $\lambda\lambda$4959, 5007, and Mg II λ2800. Lines weaker than these have small enough equivalent widths to make a negligible individual contribution to the measured continuum level. Of course the sum of weak lines may serve to raise the overall continuum level by a significant amount, but no correction was made for this effect.

For the Hα, Hβ, and [O III] lines, corrections were applied to the observed flux densities assuming the rest frame equivalent width of each line was equal to the average rest frame equivalent width observed in lower redshift quasars (Neugebauer *et al.* 1979, hereafter NOBM; Soifer *et al.* 1981; Puetter *et al.* 1981). The work of Soifer *et al.* and Puetter *et al.* suggests no strong dependence of hydrogen line strengths on redshift (and hence luminosity). No luminosity dependence has been reported for the strength of [O III]. For Hα, Hβ, and [O III], the rest frame equivalent widths were taken to be 300, 100, and 50 Å respectively. For Hα and Hβ the line width was assumed to be 10,000 km s^{-1} (full width at zero intensity), while the [O III] lines were assumed to be quite narrow. A correction was made for contributions of the Mg II line in the 1.2 μm flux density for quasars having redshifts $z > 3.1$. The maximum correction to the continuum flux for those quasars affected by the line is expected to be less than 10%. This correction is made uncertain by the possible luminosity dependence of the equivalent width of Mg II noted by Baldwin *et al.* (1978). Because of this, a correction was applied only for two quasars, whose rest frame Mg II λ2800 equivalent width is predicted, on the basis of results of Baldwin *et al.*, to be $\gtrsim$30 Å.

No attempt has been made to estimate an uncertainty associated with the corrections in Table 2 since the corrections were made for an average quasar emission-line spectrum, and there is significant variation among the quasars. Continuum flux densities for wavelengths longer than Lyα from the multichannel spectrophotometry and infrared photometry corrected for emission-line contributions are shown in Figure 1. Where variability is suggested, the energy distribution plotted in Figure 1 is that at a single epoch, with the visual and infrared data separated by the minimum time available. For comparison, the energy distribution of 3C 273 (Boggess *et al.* 1979) over the same rest frame wavelength range is also shown.

TABLE 3

PHOTOMETRY OF SUSPECTED VARIABLE QUASARS

Object	Date	1.2 μm	1.6 μm	2.2 μm
0758+12	1980 Feb	>17.44	17.49 $\pm$ 0.18	17.26 $\pm$ 0.15
	1981 Oct	17.77 $\pm$ 0.11	17.34 $\pm$ 0.10	16.66 $\pm$ 0.14
	1981 Nov	17.77 $\pm$ 0.12	17.53 $\pm$ 0.14	16.79 $\pm$ 0.19
χ^2	...	...	...	9.0
2351−154	1980 Jul	>16.88	16.40 $\pm$ 0.17	15.84 $\pm$ 0.13
	1981 Oct	16.25 $\pm$ 0.07	15.59 $\pm$ 0.06	14.67 $\pm$ 0.08
	1981 Nov	16.12 $\pm$ 0.08	15.28 $\pm$ 0.07	14.34 $\pm$ 0.08
χ^2	...	...	39.9	97.2

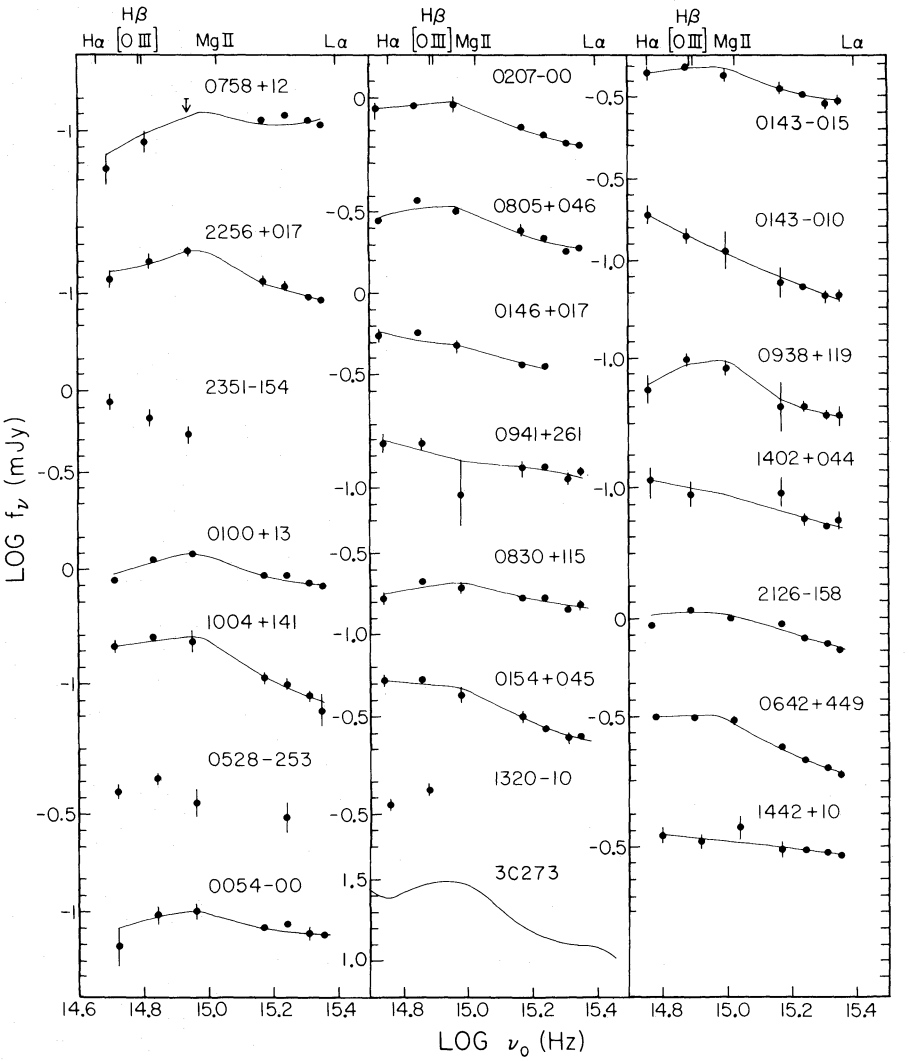

FIG. 1.—The flux densities for high-redshift quasars plotted vs. rest frequency for each object. The infrared observations are corrected, where necessary, for the presence of the emission lines noted at the top of the figure. Included for comparison is the continuum energy distribution of 3C 273. The line through the data for each quasar is the best fit model of a 3000 Å bump and power-law continuum as described in the text.

IV. DISCUSSION

The quasars observed represent roughly half of those known with redshifts $z \geq 2.66$; thus the results obtained here are probably representative of high-redshift quasars as a whole. The high-redshift nature of the sample means the quasars in the sample will be of intrinsically high luminosity. Indeed, the two highest luminosity objects in this sample, 0100+130 (PHL 957) and PKS 2126−158, are among the most luminous quasars known. Table 4 contains estimates of the luminosity at rest frame wavelengths of 0.17 and 0.41 μm. Figure 2 shows histograms of distributions of the luminosities of the present sample. The range in luminosities includes $2.1 < L_U < 34 \times 10^{12}\ L_\odot$ at ultraviolet wavelengths (0.17 μm) and $1.2 < L_O < 21 \times 10^{12}\ L_\odot$ at visual wavelengths (0.41 μm). In each case the luminosity was approximated by the product $\nu_0 F_{\nu_0}$, where F_{ν_0} is the emitted power density at the rest frequency ν_0. In this discussion, the wavelengths referred to are, unless otherwise specified, quasar rest frame wavelengths, and the continuum spectral indices and luminosities have been calculated using the flux densities corrected for line emission, as previously described. In estimating these luminosities H_0 was taken to be 50 km s^{-1} Mpc^{-1} with q_0 taken to be +1; these values were taken for ease of comparison with the results of NOBM.

The observed range in luminosities overlaps the more luminous half of the quasar sample studied by NOBM. The histograms of luminosities (Fig. 2) show, however, that many of the quasars in this sample are comparable to or less luminous than 3C 273, so the sample studied is not exclusively ultra-high-luminosity objects. The

TABLE 4

DERIVED PROPERTIES OF HIGH-REDSHIFT QUASARS

Object	Selection (Optical/Radio)	z	α_{UO}	f_B/f_C	χ^2/N	α_{OX}	$\nu_0 F\nu_0$ at log ν_0 = 15.24 $L_U(10^{12}\ L_\odot)$	$\nu_0 F\nu_0$ at log ν_0 = 14.86 $L_O(10^{12}\ L_\odot)$	L_U/L_O
0054−00	R	2.795	−0.05	0.32	1.2	< −1.66	2.8	1.2	2.3
0100+13	O	2.690	−0.10	0.42	1.2	< −1.66	31.0	16.0	1.9
0143−015	O	3.14	−0.27	0.29	0.5	< −1.52	14.0	8.6	1.6
0143−010	O	3.16	−0.89	−0.05	0.4	< −1.33	2.8	2.5	1.1
0146+017	O	2.91	−0.43	0.10	1.2	< −1.63	14.0	9.2	1.5
0154+045	O	2.99	−0.57	0.29	1.0	...	10.0	8.9	1.1
0207−003	O	2.84	−0.35	0.36	0.6	...	22.0	14.0	1.6
0528−25	R	2.765	...	...	...	...	11.0	7.9	1.4
0642+449	R	3.402	−0.56	0.36	0.5	−1.19	7.7	6.0	1.3
0758+12	R	2.660	+0.31	0.49	4.6	...	3.9	1.5	2.6
0805+046	R	2.877	−0.31	0.42	2.9	−1.39	8.1	5.9	1.4
0830+115	R	2.974	−0.11	0.29	2.0	< −1.25	6.6	3.5	1.9
0938+119	R	3.190	−0.29	0.79	0.9	< −1.26	2.1	1.8	1.2
0941+26	R	2.910	−0.35	−0.10	1.4	...	5.1	3.1	1.6
1004+141	R	2.707	−0.51	0.58	0.5	...	3.4	2.9	1.2
1320−10	O	3.14	...	...	...	...	...	7.9	...
1402+044	R	3.202	−0.49	0.05	0.6	−1.37	2.5	1.6	1.6
1442+101	R	3.53	−0.23	0.00	0.5	−1.38	15.0	6.9	2.2
2126+158	R	3.27	−0.32	0.24	3.9	−1.22	34.0	21.0	1.6
2256+017	R	2.663	−0.25	0.58	0.7	...	3.6	2.3	1.6
2351−15	R	2.665	...	...	...	...	...	7.7	...

NOTE.—All parameters are calculated with correction made for presence of emission lines in photometric band. Uncertainties are ±0.05 in α_{UO} and ±0.1 in f_B/f_C.

visually and radio-selected quasars span the same range of ultraviolet luminosities; this shows that the limiting magnitudes for the visual searches and radio identification programs are quite similar.

Finally, Figure 2 shows the histogram of the ratio L_U/L_O, i.e., the ratio of L_U, the luminosity at 0.17 μm, to L_O, the luminosity at 0.41 μm. The mean value of this ratio is 1.6, and in no case is the ratio less than 1.1. Thus, this sample of quasars is indeed a sample of ultraviolet-bright quasars, i.e., quasars which are more luminous at ultraviolet wavelengths than at other observed wavelengths. NOBM have shown that in many low-redshift quasars there is a peak in the power emitted around 3 μm. It would thus be interesting to study the rest frame infrared properties of the current sample of high-redshift quasars to see if a similar peak occurs in these quasars. Unfortunately, current instrumental sensitivities preclude a significant program of such observations.

The continuum shapes displayed in Figure 1 show a wide variety of behavior that is rarely characterizable by a simple power law. Many show a maximum in the continuum between 0.3 and 0.4 μm and have a general convex energy distribution with the slope steepening with increasing frequency. The variety in the observed continua is quite similar to that found by NOBM in the sample of low-redshift quasars.

We have attempted to fit the continuum flux densities as the sum of a power law, $f_\nu \propto \nu^\alpha$, and a "bump" centered at 0.31 μm which represents the 3000 Å excess that has been previously studied by several authors (e.g., Baldwin 1975; Grandi and Phillips 1980; NOBM; Puetter *et al.* 1982; Grandi 1982; Malkan and Sargent 1982). For this fitting, the multichannel continuum flux densities at rest frequencies corresponding to log ν_0 = 15.17, 15.24, 15.31, and 15.35 and the infrared observations corrected for the presence of the strongest emission lines were used; the multichannel frequencies were chosen so the continua were free of emission lines. The adopted shape of the 3000 Å bump was derived from the continuum energy distribution of 3C 273 as reported by Boggess *et al.* (1979) by assuming the bump was the excess flux over the power law fitted between 5586 Å and 1600 Å. The amplitude of the 3000 Å excess is described by the ratio of f_B, the flux density of the bump, at its peak wavelength, 0.31 μm, to f_C, the flux density of the power-law component at the same wavelength. This 3000 Å bump is clearly the sum of components that have been studied in detail by several authors (e.g., Grandi 1982; Puetter *et al.* 1982; Malkan and Sargent 1982; Oke, Shields, and Korycansky 1982). The adopted shape agrees well with that found by Oke, Shields, and Korycanski (1982). The best fit parameters of α_{UO} and of f_B/f_C are given in Table 4, and histograms of their distributions are given in Figure 3. The uncertainties in the model parameters are roughly ±0.05 in α_{UO} and ±0.1 in f_B/f_C.

Eighteen quasars have enough observations to be fitted. For these as a group, the power law plus bump gave a vastly superior fit than the fit with a power law only. For 15 quasars, the model gave statistically satisfactory fits to the observations. For 2126−158, 0805+046, and 0758+12, no simple model gave a satisfactory fit to the observations. In the two cases where

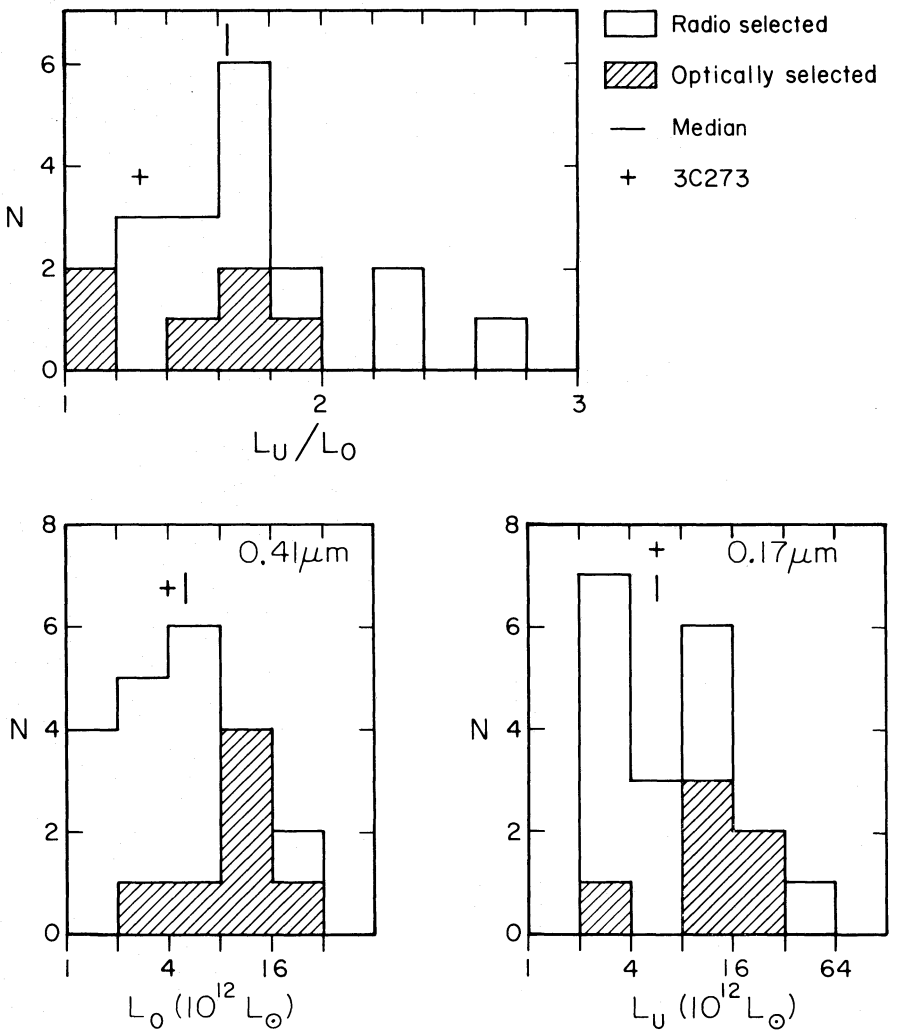

FIG. 2.—Histograms of the luminosities and the ratio of luminosities of the sample of quasars at ultraviolet and visual wavelengths. The visually and radio-selected quasars are indicated separately, as is the median of the entire sample. The value of the appropriate quantity for 3C 273 is also shown in the plots.

the model formally resulted in negative amplitudes for the bump, the bump amplitudes were consistent within the uncertainties with zero amplitude. The success of the simple model suggests that at the resolution of these observations a more complex spectral structure is not required to describe the visual/ultraviolet continua of these quasars.

The mean spectral index from visual through ultraviolet wavelengths of this sample of high-redshift quasars is -0.37 ± 0.05. This mean spectral index is in good agreement with the spectral index $\alpha = -0.5 \pm 0.1$ found by Richstone and Schmidt (1980) for a large sample of quasars with a large range of redshifts. The mean bump to continuum ratio f_B/f_C is 0.30 with a dispersion of 0.20.

From the data of Boggess *et al.* (1979), the spectral index α_{UO} of 3C 273 is -0.54 ± 0.05, and the bump to continuum ratio f_B/f_C is 0.7 ± 0.1. The spectral index of 3C 273 is well within the range of α_{UO} found for the high-redshift quasars, while the strength of the bump in 3C 273 is somewhat greater than the mean bump amplitude although within the range found for the high-redshift sample. The success of the model fits, using the bump excess defined from the 3C 273 data, and the fact that the range of parameters derived from the high-redshift samples encompasses 3C 273 argue that at this resolution the ultraviolet/visual continua of the high-redshift quasars are similar to that of 3C 273, and by inference to the continua of other low-redshift quasars, since 3C 273 is archetypical of this class of objects.

Oke and Korycansky (1982) have defined a spectral index α_{UO} between 2000 and 1200 Å from the observations of many of the quasars of this sample. They find a mean value $\alpha_{UO} = -0.49 \pm 0.04$. There is thus a suggestion of a steepening of the power-law continuum at shorter wavelengths. This marginal steepening is

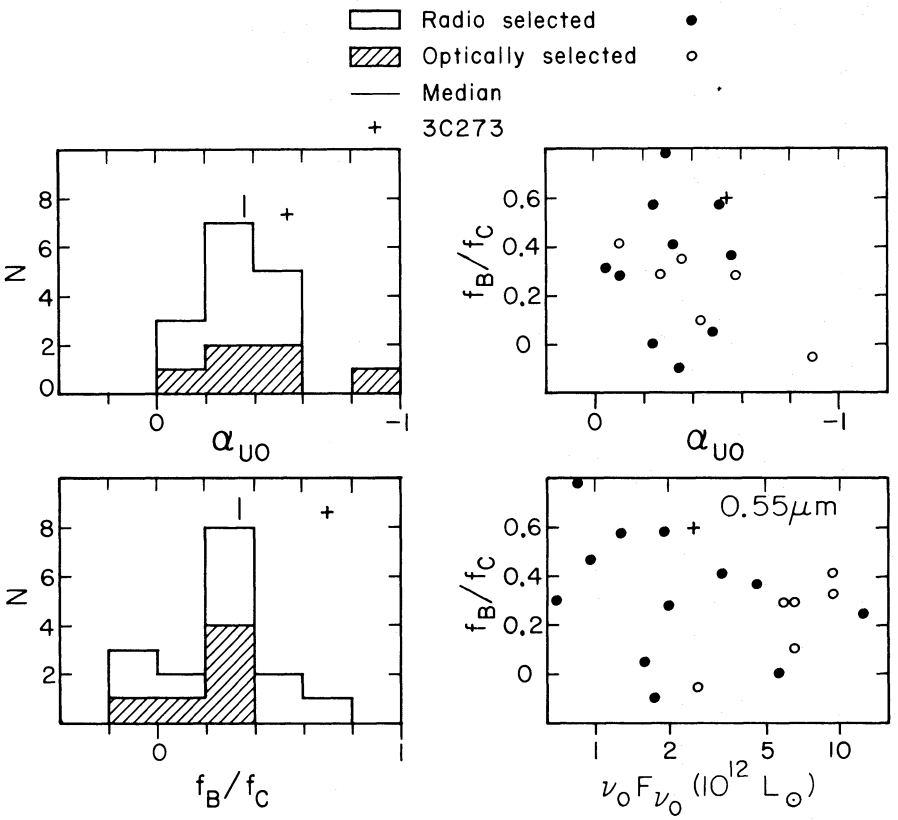

FIG. 3.—The histograms of α_{UO}, the spectral index, and of f_B/f_C, the ratio of the bump flux density to the power-law continuum flux density at 0.31 μm for the high-redshift quasars. The visually and radio-selected quasars are indicated separately, and the values of these quantities for the median of the entire sample and for 3C 273 are shown in the figure. Also plotted are the ratio f_B/f_C vs. spectral index α_{UO} and f_B/f_C vs. $\nu_0 F_{\nu_0}$, the luminosity at 0.55 μm for the observed quasars. The visually and radio-selected quasars are indicated by separate symbols, as is 3C 273.

significantly less than that derived by Cheney and Rowan-Robinson (1981) from an analysis of the Hewitt-Burbidge catalog (1980).

A search was made for correlations between the various parameters of the model fit. None was found. In particular, as shown in Figure 3, there is no correlation between the power-law slope and the strength of the bump. It is also seen in Figure 3 that there is no obvious correlation of bump excess with luminosity, although Malkan and Sargent (1982) have suggested that the strength of the 3000 Å bump is correlated with luminosity for quasars and other active galactic nuclei.

Eleven of the quasars observed in the present sample have been observed with the *Einstein Observatory* at X-ray wavelengths by Zamorani *et al.* (1981) and Ku, Helfand, and Lucy (1980); five of these, all radio-selected quasars, were detected at X-ray wavelengths. For the latter sample of five quasars, there is no correlation between α_{UO} and α_{OX}, the visual/X-ray spectral index. The mean α_{OX} of these five quasars is -1.31, while the mean α_{UO} of the same quasars is -0.35. Clearly, a significant steepening of the quasar spectra must occur at wavelengths shortward of the observed ultraviolet wavelengths. For two cases where high-resolution spectra are available, Oke and Korycansky (1982) showed that the steepening did not begin at least until the Lyman jump was reached. *International Ultraviolet Explorer* (*IUE*) observations of the high-redshift quasar Q2204−408 by Wilson, Carnochan, and Gondhalekar (1979) give a spectral index between 1500 and 400 Å of -1.5, which suggests a steepening slope below 900 Å. Observations of PG 1115+080 with *IUE* by Green *et al.* (1980) show a similar effect.

There is no evidence in these observations for different continuum properties among the visually and radio-selected quasars in the sample. This is illustrated by the histograms of Figure 3, which show that both visually and radio-selected quasars span the full range of the spectral index, α_{UO}, and of the bump to continuum ratio f_B/f_C. Thus, to the level at which the visual identification of the radio sample did not introduce a bias in the visual properties of the radio sample, no differences exist in the continuum properties at ultraviolet and visual wavelengths between the visually and radio-selected quasars observed here.

V. SUMMARY

A photometric/spectrophotometric study of 21 high-redshift quasars in the observed wavelength range

0.3–2.2 μm (rest wavelength range $\sim$800–5500 Å) has led to the following conclusions:

1. The visual/ultraviolet continuum distributions of the high-redshift quasars are fitted adequately by a sum of a power-law continuum and a 3000 Å bump excess similar in shape to that found in 3C 273.

2. Overall, the high-redshift quasars in this sample have very similar rest frame visual/ultraviolet continuum properties which are similar to those of the archetypical quasar 3C 273.

3. There is no correlation apparent between the visual/ultraviolet spectral index and the visual/X-ray spectral index for the five high-redshift quasars detected at X-ray wavelengths.

4. The visual/ultraviolet continuum properties of this sample of quasars show no correlations with selection technique (i.e., radio versus visual selection).

We thank J. Carrasco and K. Sellgren for help with the observations. Infrared research at Caltech is supported by grants from NSF and NASA. The research of J. B. O. is supported by NASA grant NSG 05-002-134.

REFERENCES

Baldwin, J. A. 1975, *Ap. J.*, **201**, 26.
Baldwin, J. A., Burke, W. L., Gaskell, C. M., and Wampler, E. J. 1978, *Nature*, **273**, 431.
Boggess, A., *et al.* 1979, *Ap. J.* (*Letters*), **230**, L131.
Cheney, J. E., and Rowan-Robinson, M. 1981, *M.N.R.A.S.*, **195**, 831.
Grandi, S. A. 1982, *Ap. J.*, **255**, 25.
Grandi, S. A., and Phillips, M. M. 1980, *Ap. J.*, **239**, 475.
Green, R. F., Pier, J. R., Schmidt, M., Estabrook, F. B., Lane, A. L., and Wahlquist, H. D. 1980, *Ap. J.*, **239**, 483.
Hewitt, A., and Burbidge, G. 1980, *Ap. J. Suppl.*, **43**, 57.
Ku, W., Hefland, D., and Lucy, L. 1980, *Nature*, **288**, 323.
Kunth, D., Sargent, W. L. W., and Kowal, C. 1981, *Astr. Ap. Suppl.*, **44**, 229.
MacAlpine, G. M., and Lewis, D. W. 1978, *Ap. J. Suppl.*, **36**, 587.
MacAlpine, G. M., Smith, S. B., and Lewis, D. W. 1977, *Ap. J. Suppl.*, **35**, 197.
Malkan, M., and Sargent, W. L. W. 1982, *Ap. J.*, **254**, 22.
Neugebauer, G., Oke, J. B., Becklin, E. E., and Matthews, K. 1979, *Ap. J.*, **230**, 79 (NOBM).
Oke, J. B., and Korycansky, D. G. 1982, *Ap. J.*, **255**, 11.
Oke, J. B., Shields, G. A., and Korycansky, D. G. 1982, in preparation.
Puetter, R. C., Burbidge, E. M., Smith, H. E., and Stein, W. A. 1982, *Ap. J.*, **257**, 487.
Puetter, R. C., Smith, H. E., Willner, S. P., and Pipher, J. L. 1981, *Ap. J.*, **243**, 345.
Richstone, D. D., and Schmidt, M. 1980, *Ap. J.*, **235**, 377.
Smith, H. E., Jura, M., and Margon, B. 1979, *Ap. J.*, **228**, 369.
Soifer, B. T., Neugebauer, G., Oke, J. B., and Matthews, K. 1981, *Ap. J.*, **243**, 369.
Wilson, R., Carnochan, D. J., and Gondhalekar, P. M. 1979, *Nature*, **277**, 457.
Zamorani, G., *et al.* 1981, *Ap. J.*, **245**, 357.

J. B. Oke: Division of Physics, Mathematics, and Astronomy, Robinson Laboratory 105–24, California Institute of Technology, Pasadena, CA 91125

J. H. Lacy, K. Matthews, G. Neugebauer, and B. T. Soifer: Division of Physics, Mathematics, and Astronomy, Downs Laboratory 320–47, California Institute of Technology, Pasadena, CA 91125